Molecular Catalysis 476 (2019) 110484

Contents lists available at ScienceDirect

Molecular Catalysis

journal homepage: www.elsevier.com/locate/mcat

Development of novel support for penicillin acylase and its application in 6-aminopenicillanic acid production

Sonal R. Ayakar, Ganapati D. Yadav*

Department of Chemical Engineering, Institute of Chemical Technology, Nathalal Parekh Marg, Matunga, Mumbai, 400 019, India

ARTICLE INFO

Keywords:
Penicillin acylase
6-Aminopenicillanic acid
Enzyme entrapment
Polyvinyl alcohol-alginate beads
Mesocellular foam silica (MCF)

ABSTRACT

There is an ever-increasing demand for the β-lactam bulk intermediate 6-aminopenicillanic acid (6-APA) that has wide applications in the synthesis of newer generations of semisynthetic penicillins. It is commercially synthesized by biocatalytic transformation using penicillin acylase. Since the enzyme is soluble, immobilization on a solid porous support is necessary to make the catalyst recycleable and the process profitable. In this study, we developed a novel support of siliceous foam entrapped in a polymer matrix. Penicillin acylase was covalently immobilized on aminopropyl functionalized mesocellular foam silica (MCF) and was further cross-linked using glutaraldehyde without deactivation and upto 95% efficiency. The resulting biocatalyst had an activity of 1185 IU. mg^{-1} and demonstrated improved resistance to the substrate and product inhibition. These parameters along with improvement in pH and thermal stability enhanced 6-APA yield by 20% in beads. Intrinsic kinetic parameters were calculated from the developed rate equation to deduce enzyme catalytic mechanism.

1. Introduction

A β-lactam bulk intermediate, 6-aminopenicillanic acid (6-APA) is used in the synthesis of newer generations of semisynthetic penicillin [1,2]. 6-APA is synthesized from penicillin G or penicillin V by side chain hydrolysis. There are two routes for 6-APA synthesis. The entirely chemical route was used until the 1980s known as 'Delft cleavage' [3]. This route posed several sustainability hazards and lost its popularity due to the involvement of hazardous chemicals, reactions conducted at very low temperatures; and generation of hazardous waste [4]. The second route is a single step enzymatic transformation using microbial penicillin acylase in an aqueous environment [5]. Efficient enzyme production and recovery have aided the successful implementation of biocatalysis for 6-APA synthesis. Despite these advantages, the soluble nature of the enzyme, penicillin G and co-products – 6-APA and phenylacetic acid (PAA) make enzyme reuse and product purification difficult. Though penicillin acylase is a very well studied class of enzymes, it suffers from various stability issues. Wild type enzyme lacks thermal stability and wide pH activity [6]. The reaction of 6-APA formation is reversible and hence it is difficult to reach 100% conversion (Scheme 1). The products PAA and 6-APA inhibit the enzyme further reducing the enzyme activity [7]. These problems are eliminated or dealt by immobilizing the enzyme and recovery as heterogeneous phase [8–13]. A continuous reactor system has also been investigated [14,15]. Techniques of immobilization on gels, films, foams, beads, and porous materials as well as microbial aggregates have been reported. The most recent advancements in PGA immobilization strategy have been in the selection of mode and support for immobilization. One approach that is gaining popularity is the employment of thermo-sensitive block copolymers. They provide an advantage of carrying out the catalysis at the solution stage and raising temperature beyond lower critical solution temperature (LCST) to cement the polymer with an enzyme for separation. The polymers studied for PGA bear LCST of 39 °C [16] which is lower than optimal temperature (above 40 °C) observed for PGA activity [17]. Magnetic supports have been studied for PGA immobilization that offer ease of separation post reaction [17–21]. The iron oxide-based supports suffer from low surface area and pore volume limiting enzyme loading capacity [17]. To impart higher porosity to the support structure various other template-based approaches have been attempted [19] wherein, the immobilization ceiling point was reached by the highest reported surface area (323 $m^2.g^{-1}$). Moreover, the magnetic support particles show high-degraded reactivity, which leads to their instability and aggregation [22]. Silica has been extensively studied as the support material for PGA immobilization [23–26] due to its hydrophilic nature and ease of surface modification. Particulate silica shows lower surface area leading to very low activity retention and reusability. One such approach involving adsorption, crosslinking and covalent linking led to activity recovery of maximum 62% [23].

* Corresponding author.
E-mail addresses: gdyadav@yahoo.com, gd.yadav@ictmumbai.edu.in (G.D. Yadav).

https://doi.org/10.1016/j.mcat.2019.110484
Received 24 February 2019; Received in revised form 15 June 2019; Accepted 20 June 2019

Nomenclature

A	penicillin G
B	water
P	6-APA
D	PAA
E	are active sites on the biocatalyst
C_A	concentration of A in bulk (mol. cm^{-3})
C_B	concentration of B in bulk (mol. cm^{-3})
C_P	concentration of P in bulk (mol. cm^{-3})
C_Q	concentration of Q in bulk (mol. cm^{-3})
C_P	concentration of P in bulk (mol. cm^{-3})
$C_{A.E}$	concentration of A complexed with E (mol. cm^{-3})
$C_{B.E}$	concentration of B complexed with E (mol. cm^{-3})
$C_{P.E}$	concentration of P complexed with E (mol. cm^{-3})
$C_{Q.E}$	concentration of Q complexed with E (mol. cm^{-3})
C_t	concentration of total catalytic sites on E (mol. cm^{-3})
C_E	concentration of free catalytic sites on E (mol. cm^{-3})
w	biocatalyst loading (g. cm^3)
k'	reaction rate constant for forward reaction of A and B giving P and Q (cm^3. mol^{-1}. min^{-1})
k'_1	reaction rate constant for reverse reaction of P and Q giving A and B (cm^3. mol^{-1}. min^{-1})
K_A	equilibrium constant for complexation of A with E (cm^3. mol^{-1})
K_B	equilibrium constant for complexation of B with E (cm^3. mol^{-1})
K_P	equilibrium constant for dissociation of P from E (mol. $cm-^3$)
K_Q	equilibrium constant for dissociation of Q from E (mol. cm^{-3})
k''	actual reaction rate constant for reaction of A and B (cm^3
k	apparent rate constant for reaction of A and B (min^{-1})

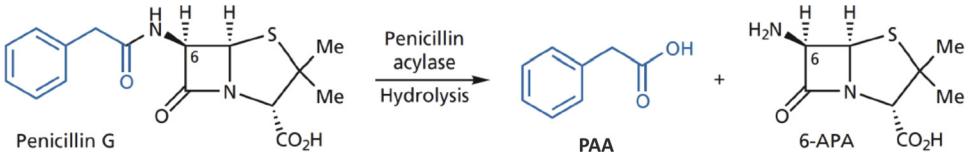

Scheme 1. Enzymatic hydrolysis of penicillin G to 6-aminopenicillanic acid (APA) and phenylacetic acid (PAA).

In this study we selected MCF as a porous support for immobilization due to its high surface area and pore volume available for penicillin G acylase (PGA). PGA is a large periplasmic protein with a high molecular weight (86 kDa) and 7 nm × 50 nm × 5.5 nm in size. The active site is located deep inside the PGA structure at the bottom of cone-shaped depression formed by intertwining of the two chains of the enzyme molecule [27]. PGA demonstrates attraction for electronegative groups through common surface amino acid residues like tyrosine, arginine, histidine, lysine, serine and threonine. The effects of nature of porous supports for PGA immobilization [9,25,28] and pore characteristics [28] have been studied in detail. Higher pore size and pore volume were demonstrated to improve PGA immobilization [28]. The choice of porous support was based on its having suitable surface and pore characteristics to provide accommodation and formation of a monolayer of PGA. Ordered mesoporous silica has well controlled and uniformly sized pores ranging from 2 to 50 nm; synthesized by the intelligent arrangement of the block copolymer (or organic surfactant) and an inorganic silica source and are employed in enzyme immobilization [29]. Mesocellular foam silica (MCF) among these has tunable > 15 nm pores making it a suitable candidate as support for penicillin acylase [30]. MCF has been reported as good support for various biocatalytic applications [24,31,32]. Another advantage of employing MCF as support is its flexibility towards surface modification due to the reactive chemistry of silanol groups [29]. It can be used directly for immobilization aided by adsorption or coupled with various techniques like covalent binding or crosslinking. The covalent binding provides selective and stronger interactions without substantially altering the diffusional properties of the foam. PGA has exhibited interactions with aminopropyl functionalized foam [25]. This work involves the development of an efficient immobilization strategy to tackle these issues and to optimize the bioprocess through enzyme kinetic studies. It provides a comparative study of different modes of immobilization on MCF. We employed PGA immobilization by covalent attachment on amino-modified MCF followed by glutaraldehyde crosslinking to achieve stronger binding. It led to high enzyme loading and activity retention but lost the enzyme by leaching through repeated use. To combat this, the pore size of MCF could not be reduced as it has shown to lower the enzyme loading in the past [33]. Increasing the crosslinking also negatively impacted the enzyme activity due to loss of flexibility [34–36]. Entrapment in the polymeric matrix has not only reported to prevent enzyme leaching but also to improve enzyme stability through micro-environment regulation [36–39]. Hence, the final step of entrapment was integrated, and the resulting biocatalyst showed improved reusability. We also developed a new kinetic model that can predict the reaction course and parameters.

2. Materials and methods

2.1. Enzyme and reagents

Penicillin G acylase (PGA, EC 3.5.1.11) was obtained as a gift sample from KDL Biotech Ltd., India in phosphate buffer (pH 7.5). The source organism of the enzyme is *E. coli*. Penicillin G potassium salt was procured from Unimark Remedies, India. Chemicals involved in MCF support synthesis were tetraethyl orthosilicate (TEOS, Merck, India), Pluronic P123 triblock copolymer (poly (ethylene oxide)-block–poly (propylene oxide)-block-poly (ethylene oxide), EO20–PO70–EO20, MW = 5800) (Sigma Aldrich, India), 1,3,5-trimethylbenzene (TMB)/ mesitylene (Sigma Aldrich, India), ammonium fluoride (Thomas Baker, India), 3-aminopropyltriethoxysilane (APTS) (Sigma Aldrich, India), glutaraldehyde 25% w/v aqueous solution (SDFCL, India) and hydrogen chloride 37% w/v aqueous solution (Sigma Aldrich, India). Chemicals used for entrapment were sodium alginate and polyvinyl alcohol (S.D. Fine Chemicals, Mumbai India), gelatine and starch (Himedia, Mumbai), calcium chloride, boric acid potassium dihydrogen phosphate, dipotassium hydrogen phosphate and tris HCl (all Sigma Aldrich, India). Buffers were suitably prepared in deionized water.

2.2. MCF synthesis and amino-functionalization

MCF was prepared by the hydrothermal method [32]; 2 g of pluronic P123 was dissolved in 75 cm^{-3} of 1.6 M aqueous hydrochloride solution at room temperature. 4 g of TMB was then added and the resulting solution was stirred vigorously at 39 °C for 3 h. 4.6 cm^3 of TEOS was added to the mixture and stirring was continued for 24 h. 2.5 cm^3 of 0.27 M aqueous ammonium fluoride solution was then added, and the resulting mixture was kept at 100 °C for 30 h for aging. The white solid obtained was filtered and washed with deionized water

until the filtrate was neutral. It was again washed thrice with ethanol, dried at 100 °C for 12 h and calcined at 550 °C for 6 h. 0.25 g of APTS was added to 200 cm^3 of 1 M aqueous hydrochloride solution at room temperature and was stirred for hydrolysis. 1 g of MCF was added to it and the mixture was shaken in an incubator shaker at 25 °C for 8 h at 160 rpm. The suspension obtained was then kept at 100 °C for 24 h. The resulting powder was filtered and washed with water and ethanol. It was dried at 80 °C for 12 h. This product is labeled as NH_2-MCF.

2.3. Enzyme crosslinking and entrapment

0.2 *g* of NH_2-MCF was mixed with 10 cm^3 of 0.05 M phosphate buffer of pH 7.9 and wetted under shaking for 1 h. PGA was added to the mixture and shaken in an incubator shaker at 25 °C or 3 h at 200 rpm. This stage was designated as Enz-NH_2-MCF. To the same suspension, glutaraldehyde solution was added, and shaking was continued for one more hour. The solid obtained was centrifuged and washed several times with phosphate buffer (0.05 M, pH 7.9) till supernatant was free of protein (confirmed by Bradford protein assay). The product obtained was named as Crs-Enz-NH_2-MCF. Effect of concentration of glutaraldehyde was tested from 0.05 M to 0.2 M. For entrapment into beads, 5 cm^3 Crs-Enz-NH_2-MCF was mixed with 10 cm^3 polymer solution and the resulting suspension was filled in a syringe fitted with 22 G × 1¼" (0.7 mm × 30 mm) needle. Beads were cast by controlled release of the suspension in chilled congealing solution from a height of 15 cm. The beads obtained were cured in the same solution for 12 h at 4 °C. Beads were then filtered and washed several times with water.

Alginate and its composites with starch, gelatine and polyvinyl alcohol (PVA) were tested of physical stability using NH_2-MCF foam as a

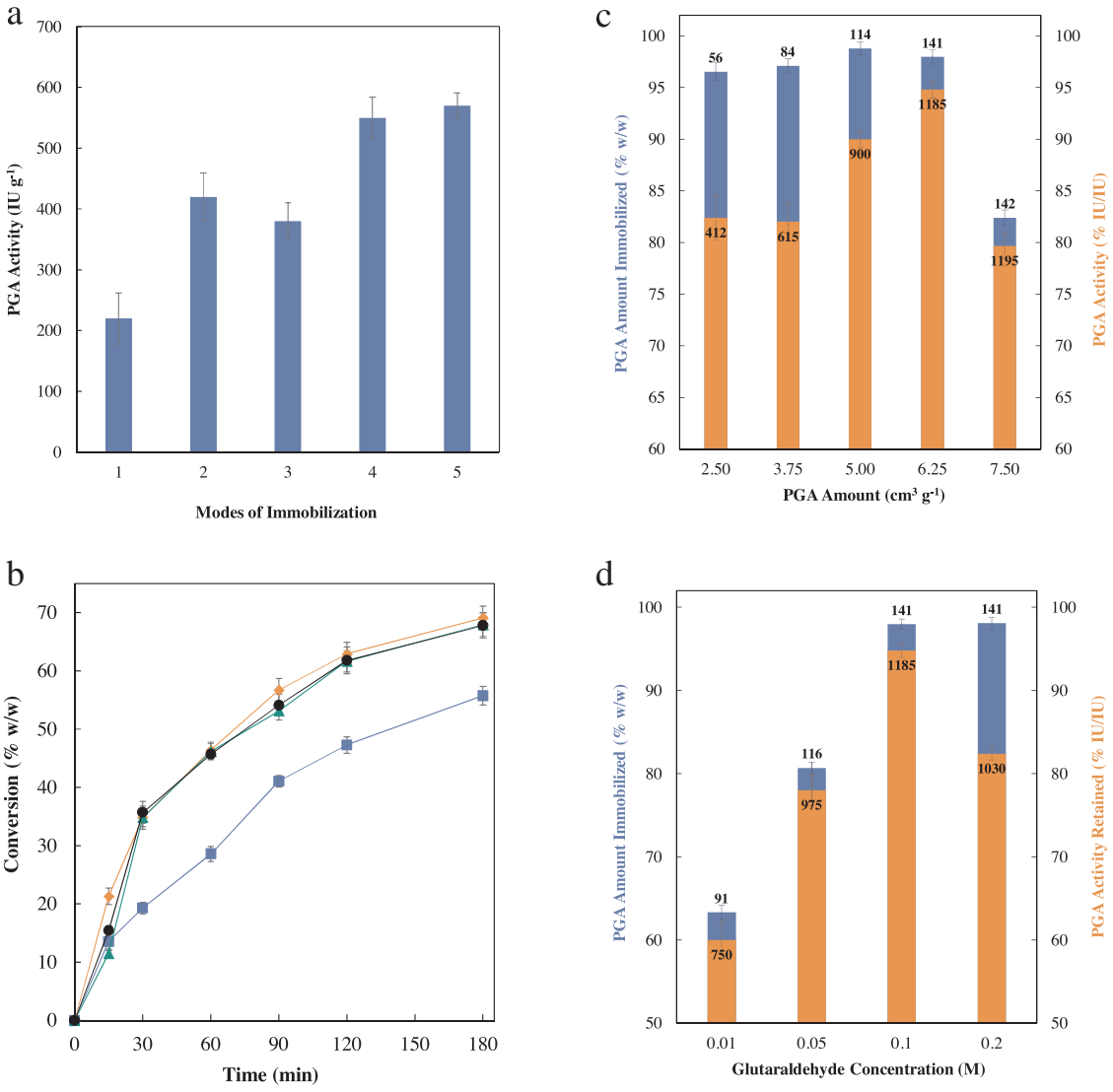

Fig. 1. (a) Effect of modes of penicillin G acylase immobilization on activity. 1: adsorption on mesocellular foam (MCF), 2: adsorption on MCF followed by glutaraldehyde crosslinking (Crs-Enz-MCF), 3: covalent attachment on aminopropyl functionalized MCF (Enz-NH_2-MCF), 4: covalent attachment on aminopropyl functionalized MCF followed by glutaraldehyde crosslinking (Crs-Enz-NH_2-MCF), 5: covalent attachment on aminopropyl functionalized MCF followed by glutaraldehyde crosslinking and subsequent entrapment in alginate-polyvinylchloride beads (SA/PVA-Crs-Enz-NH_2-MCF). (b) Effect of support matrix on penicillin G acylase activity on immobilization and time course study. ■ Free enzyme, ◆ Crs-Enz-NH_2-MCF, ● SA/PVA-Crs-Enz-NH_2-MCF, ▲ Permeabilized SA/PVA-Crs-Enz-NH_2-MCF. (c) Effect of enzyme loading on PGA immobilization as Crs-Enz-NH_2-MCF. ■ Percent penicillin G acylase amount retained on immobilization (data label shows value in mg of protein immobilized per g of the support), ■ percent penicillin G acylase activity retained on immobilization (data label shows value of activity obtained in IU per g of the support). (d) Effect of glutaraldehyde comcentration on PGA immobilization as Crs-Enz-NH_2-MCF. ■ Percent penicillin G acylase amount retained on immobilization (data label shows value in mg of protein immobilized per g of the support), ■ percent penicillin G acylase activity retained on immobilization (data label shows value of activity obtained in IU per g of the support).

control. Detailed protocols for making individual beads were: a) alginate beads- sodium alginate (SA) solution in water congealed with 0.2 M calcium chloride solution; b) SA/starch beads- 2% (w/v) SA and 10% (w/v) starch (gelatinized at 70 °C) and congealed with 0.2 M calcium chloride solution; c) SA/gelatine beads- 2% (w/v) SA and 10% (w/v) gelatine (gelatinized at 70 °C) and congealed with 0.2 M calcium chloride solution; d) SA/PVA 1–2 % (w/v) SA and 2–10 % (w/v) PVA (gelatinized at 70 °C) and congealed with 0.2 M calcium chloride and 0.5 M boric acid solution. Permeabilization of beads was carried out by washing them with phosphate buffer (0.05 M pH 8) and water. They were then hardened in the congealing solution for 1 h prior to air drying and stored at 4 °C until use.

2.4. Protein quantification and enzyme assay

The protein content was determined by Bradford protein assay (bovine serum albumin was used to plot a standard calibration curve). Enzyme activity assay was performed as reported [25].

2.5. Characterization of immobilized PGA

FT-IR studies were conducted for MCF, NH_2-MCF, Crs-Enz-NH_2-MCF to analyze functionalization by using a Bruker IFS-66 single-channel Fourier transform spectrophotometer. The thin pellet was prepared by mixing the sample with spectroscopic grade potassium bromide. The pellet was subjected to a number of scans to record the spectra from 4000 cm^{-1} to 400 cm^{-1}. XRD analysis was carried out on Bruker diffractometer D8 with Cu-Kα (1.54 Å) radiation for MCF, NH_2-MCF. The X-ray diffraction patterns were recorded in the 2θ from 5 to 50°. The surface properties were measured by the Brunauer–Emmett–Teller (BET) method using ASAP 2020 (Micromeritics, USA). Degassing was necessary prior to analysis with conditions: MCF (at 623 K for 4 h); NH_2-MCF (at 373 K for 4 h); Crs-Enz-NH_2-MCF, PVA/SA-Crs-Enz-NH_2-MCF and permeabilized PVA/SA-Crs-Enz-NH_2-MCF (at 323 K for 6 h). Morphological characteristics of MCF, NH_2-MCF, Crs-Enz-NH_2-MCF and PVA/SA-Crs-Enz-NH_2-MCF were captured with a scanning electron microscope (Camera SU 30 microscope, JEOL, Japan). TEM was performed for the foam and the beads using JEOL JEM 2100, Japan microscope. Thermogravimetric analysis (TGA) and differential scanning calorimetry (DSC) was carried out on STA 6000 Pyris (Perkin Elmer) series analyzer. About 20 mg of sample was placed in the analyzer and the analysis was programmed from 30–200 °C with 10 °C/min rise in temperature. Crs-Enz-NH_2-MCF and PVA/SA-Crs-Enz-NH_2-MCF were analyzed by this technique.

2.6. Reaction set up and conditions

Cylindrical, flat bottom, baffled glass reactor with an aspect ratio (H/D) of 2 and of capacity 50 cm^3 was used to carry out reactions. The reactor had an internal diameter of 2 cm. A standard 6 blade-pitched turbine impeller of 0.7 cm diameter was used for stirring. The impeller was placed at a height of 0.7 cm from the bottom. The temperature of reaction mass was maintained using a thermostatic water bath with an accuracy of ± 1 °C. A typical reaction consisted of 30 cm^3 of 30 mM penicillin G potassium salt, 0.3 g PVA/SA-Crs-Enz-NH_2-MCF bead loading in phosphate buffer (10 mM, pH 7.0). The course of reaction for this study was 3 h in most of the cases. Effect of temperature was tested from 30 to 60 °C. For all the comparative experiments, activity equivalent of free PGA and immobilized PGA (on foam or in beads) was used.

2.7. HPLC analysis of the reaction mixture

The analysis was carried out by reverse phase HPLC (Agilent 1260 infinity) using Agilent Zorbax Eclipse C18 column (250 mm × 4.6 mm × 5 µm). The mobile phase composition was buffer A and acetonitrile in the isocratic elution mode in the ratio of 7:3, respectively. Buffer A contained 5 mM potassium dihydrogen phosphate and 2.4 mM sodium dodecyl sulphate, a solution of which was adjusted to pH 3 with phosphoric acid. The column temperature was maintained at 30 °C and diode array detector set at 215 nm wavelength. The retention time for penicillin G was 8.2 min, 6-APA was 4.1 min and PAA was 9.9 min. To study the hydrolysis of penicillin G to yield 6-APA various parameters (agitation, pH, temperature and substrate concentration) were studied. Enzyme kinetic analysis was also performed.

3. Results and discussion

3.1. Mode of PGA immobilization

MCF was synthesized with a gravimetric yield of 96% calculated based on the template. Aminopropyl functionalization had a gravimetric yield of 90%. Protein content and activity of the PGA solution was 23.0 $mg.cm^{-3}$ and 200 IU. cm^{-3}, respectively. The modes of PGA immobilization studied were: adsorption on MCF (Enz-MCF), adsorption on MCF followed by glutaraldehyde crosslinking (Crs-Enz-MCF), covalent binding on aminopropyl functionalized MCF (Enz-NH_2-MCF) and covalent binding on aminopropyl functionalized MCF followed by glutaraldehyde crosslinking (Crs-Enz-NH_2-MCF). For this purpose, 600 IU PGA was added to 1 g of the support and 0.1 M glutaraldehyde was used for crosslinking. Results showed that the nature of forces utilized for immobilization had a significant effect on activity (Fig. 1a). Weaker interactions of adsorption gave low protein loading and subsequent activity (26.4 mg protein loading and 220 IU g^{-1} of Enz-MCF activity). Stronger interactions of covalent binding achieved higher enzyme loading and activity (45.6 mg protein loading and 380 IU.g^{-1} of Enz-NH_2-MCF activity). Glutaraldehyde crosslinking had a positive effect on activity retention (53.0 mg protein loading and 420 IU.g^{-1} of Crs-Enz-MCF activity). Both covalent binding and crosslinking resulted in higher activity and hence was selected for further studies (67.5 mg protein loading and 550 IU.g^{-1} of Crs-Enz-NH_2-MCF activity). Reactions of penicillin G hydrolysis with Crs-Enz-NH_2-MCF lost 47% of the activity on 4th reuse. The reaction mixture was then tested for the presence of PGA by Bradford assay. The mixture showed the presence of protein and hence confirmed the loss in activity due to enzyme leaching on reuse. Crs-Enz-NH_2-MCF was entrapped into polymeric beads (SA/PVA-Crs-Enz-NH_2-MCF) to prevent PGA leaching. The entrapment caused no change in the activity (570 IU. g^{-1} of SA/PVA-Crs-Enz-NH_2-MCF activity) and retained 91% activity after 4th reuse. These results are summarized in Table 2.

The above study concluded that the entrapment improved the reusability as well as the activity of the biocatalyst. There are reports that the microenvironmental conditions around the enzyme influence its activity [36,37]. The entrapment has also reported to increase the diffusional limitations and hence a comparative study was planned to judge the influence of entrapment on the course of the reaction (Fig. 1b). These reactions were carried out at the following conditions: 6 IU PGA in 30 cm^{-3} reaction buffer pH 7 containing 10 mM penicillin G, agitated at 200 rpm and at 50 °C. The free enzyme had the lowest conversion and immobilization improved the activity of the enzyme. Crs-Enz-NH_2-MCF, SA/PVA-Crs-Enz-NH_2-MCF and permeabilized SA/PVA-Crs-Enz-NH_2-MCF reached similar substrate conversion (67% - 68%). Free enzyme reached 56% conversion in 180 min. This verified that the entrapment had no substantial effect on the activity as well as mass transfer. Crs-Enz-NH_2-MCF had the fastest initial rate (0.121 mM.min^{-1}) followed by permeabilized PVA/SA-Crs-Enz-NH_2-MCF (0.116 mM.min^{-1}) and PVA/SA-Crs-Enz-NH_2-MCF (0.108 mM.min^{-1}) suggesting time lag to set up uniform concentration profile inside the beads than that of foam. But after the achievement of uniform concentration profile in beads, the rate matched with that of the foam. Permeabilization of beads did not have an effect on conversion due to the high catalytic activity of the enzyme and the mass transfer

inhibitions were already taken care at the speed of agitation of 200 rpm.

3.2. Effect of enzyme loading

The enzyme distribution affects the specific activity of the immobilized enzyme [25]. Densely distributed enzyme molecules cannot transition easily to their active form. Hence, it was required to estimate the optimal loading and determined by varying enzyme concentration (2.5 to 7.5 cm^{-3} or 500 to 1500 IU) keeping immobilization conditions the same. The protein loading and activity went on increasing till enzyme loading of 6.25 $cm^{-3}.g^{-1}$ of NH_2-MCF beyond which it did not change. At this PGA concentration, all sites on support were saturated (Fig. 1c). Immobilization efficiency was 98% and around 3% enzyme deactivation occurred from mass balance calculations leading to 95% activity recovery. The deactivation was higher at lower enzyme loading due to excessive crosslinking by glutaraldehyde per PGA molecule. Average crosslinks per enzyme molecule determined the degree of deactivation. So, PGA loading was optimized to 6.25 $cm^3.g^{-1}$ that achieved 140 $mg.g^{-1}$ protein loading and 1185 IU. g^{-1} activity.

3.3. Effect of glutaraldehyde concentration

Lysine residues on the surface of an enzyme are involved in forming crosslinks with glutaraldehyde [34] preventing enzyme leaching. Glutaraldehyde concentration was varied from 0.01 to 0.2 M (Fig. 1d). Lower glutaraldehyde concentration leads to insufficient crosslinking leading to lower activity retention (verified by the presence of PGA in washings). Higher glutaraldehyde concentration leads to higher crosslinking resulting in loss of flexibility in the enzyme molecule required for catalytic activity [34–36]. The enzyme reached maximum immobilization efficiency at 0.1 M. At higher glutaraldehyde concentration (0.2 M), excessive crosslinking decreased PGA activity. 0.1 M glutaraldehyde was therefore employed in the later stages of work. Crs-Enz-NH_2-MCF generated as a result of these steps did leach PGA on use and hence required entrapment in a polymeric matrix.

3.4. Bead polymer stability

Polymer concentration influences two parameters – bead stability and mass transfer resistance for reactant, products and enzyme. Optimum polymer concentration will impart stability to beads, ease movement of reactant and products, but hinder escape of enzyme molecules. We tested alginate and composite polymer blends for entrapment. SA concentration was varied from 0.5 to 4 % w/w. 2% SA beads lost their shape on washings, but 4% SA beads retained their shape. When they were tested in reaction, the alginate polymer solubilized at reaction conditions. Hence SA was blended with other polymers to improve stability. Polymer SA/starch beads leached foam on storage due to starch solubilization. SA/gelatine beads had high surface instability and aggregated on storage. SA/PVA beads had better stability and were selected for further perturbations to optimize polymer blend ratio. 2% w/v SA and 5% w/v PVA led to optimal stability. Crs-Enz-NH_2-MCF trapped in these SA/PVA beads (SA/PVA-Crs-Enz-NH_2-MCF) had an activity of 20 IU. g^{-1} and exhibited higher thermal stability than Crs- Enz-NH_2-MCF (Fig. 6b). Improvement in the thermal stability of the enzyme on immobilization has been studied for PGA and other enzymes [5,31,35,40] that highlight the involvement of favourable interactions of the enzyme with the support [41]. The beads obtained were spherical (1–1.5 mm diameter) in shape and stable in 10 mM phosphate buffer at pH range from 6 to 9.

3.5. FT-IR characterization of the biocatalyst

FT-IR spectra showed (Fig. 2a) a broad peak at 3400-3300 cm^{-1} is ascribed to the O—H stretch vibrations of the Si—OH chains, whereas the peak at around 970 cm^{-1} is attributed to the O—H bend vibrations of the Si—OH chains. The peaks at 1090 cm^{-1} and 800 cm^{-1} correspond to the antisymmetrical and symmetrical stretch vibrations of the Si–O–Si bond, respectively. The peak at 460 cm^{-1} results from the Si–O–Si bend vibrations. The peaks at 1635 cm^{-1} and 3500 cm^{-1} are assigned to the bend and stretch vibrations, respectively, of the N—H bond. The spectra of NH_2-MCF showed a drop in transmittance at 1650 cm^{-1} and 3500 cm^{-1} indicating amino functionalization. For Crs-Enz-NH_2-MCF, there appeared shrinkage in O—H and N—H stretch (3500-3300 cm^{-1}) region indicating occupancy of the enzyme at these sites with covalent binding.

3.6. XRD analysis of the biocatalyst

Fig. 2b gives XRD patterns. A single peak was obtained at 2θ value of 22.4°. The broad nature of the peak indicates the amorphous nature of MCF, NH_2-MCF and Crs-Enz-NH_2-MCF. The full width half maximum (FWHM) was 6.0° suggesting the high degree of amorphous attitude. Reduction in the peak intensity from MCF to NH_2-MCF to Crs-Enz-NH_2-MCF was observed. The average spacing between the two layers (d) was observed to be 4.0 Å which suggest the thickness of a single cell layer of

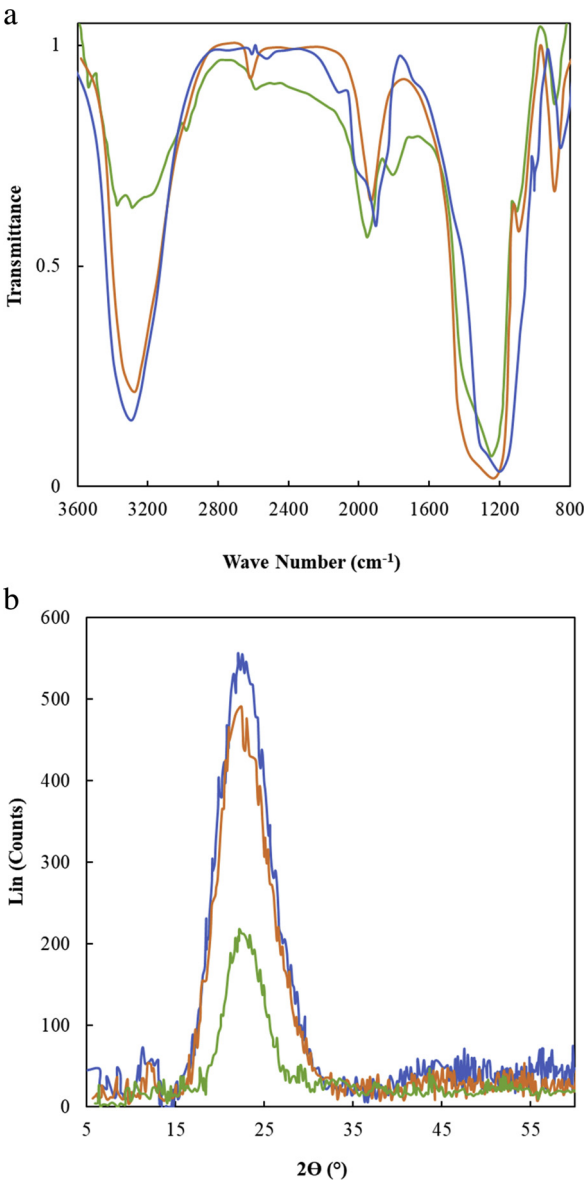

Fig. 2. (a) FT-IR spectrum of MCF, NH_2-MCF and Crs-Enz-NH_2-MCF. (b) XRD pattern of MCF, NH_2-MCF and Crs-Enz-NH_2-MCF.

mesocellular foam (MCF).

3.7. Surface and pore structure characterization of the biocatalyst

Surface property characterization using ASAP (Table 1) revealed that the MCF synthesized had a high surface area (more than 600 $m^2 g^{-1}$) with high pore volume (3.2 $cm^3. g^{-1}$) and large pore size (28 nm). Surface area decreased on aminopropyl functionalization and subsequent enzyme immobilization suggesting occupancy of the groups in pores. Aminopropylation of MCF did not alter the pore volume due to thin layer binding; but average pore size increased due to blockade of small pores. Beads had smaller pore size and hence prevented enzyme leaching. Permeabilization of the beads opened the pores due to swelling but the pore volume remained unchanged. Isotherms of all the samples showed hysteresis loop between adsorption isotherm and desorption isotherm depicting mesoporous nature.

3.8. Electron microscopic analysis of the biocatalyst

SEM images (Fig. 3a–f) of MCF and Crs-Enz-NH_2-MCF showed no difference in the surface morphology. SA/PVA-Crs-Enz-NH_2-MCF image showed a coating of SA and PVA composite matrix on the foam. The surface thus appeared bulgy and porous. To have more elaboration about the topography, high-resolution images were taken. MCF was made up of spherical particles of particle size of 3–4 μm. The spherical particles were in an agglomerated state with a smooth surface. The TEM images (Fig. 4a and b) of Crs-Enz-NH_2-MCF showed the presence of three-dimensional pore system which was composed of uniformly sized large hexagonal cells interconnected by uniform windows. The particles had defined and thick wall structure. This justifies the high adsorption properties of MCF. TEM images of SA/PVA-Crs-Enz-NH_2-MCF (Fig. 4c and d) showed a polymer coat around the foam particles. The film formed by PVA/SA composite matrix is thin and the foam is successfully entrapped into it.

3.9. Effect of speed of agitation

The substrate (penicillin G) molecules are required to reach the enzyme active site situated inside the support overcoming interparticle and intraparticle mass transfer resistance for the progress of the reaction. To ensure that the reaction was not diffusion controlled, the support porosity was kept higher. It was thus assumed that the concentration of the substrate on the surface of the supports is the same as that present inside the pores. To overcome the mass transfer limitation, an influence of speed of agitation on the progress of the reaction was studied (Fig. 5a) at a reaction temperature of 40° C. Penicillin G conversion increased with increasing agitation until 200 rpm; at speed higher than 200 rpm, the conversion remained constant. At 300 rpm, the beads underwent physical damage due to shear and a steep rise in the conversion was observed. Reusability of broken biocatalyst reduced drastically. Hence optimal agitation speed was 200 rpm.

3.10. Effect of pH

An enzyme is a polymer of amino acids and its activity is highly dependent on the pH of the solution. The activity profiles for free and immobilized PGA (SA/PVA-Crs-Enz-NH_2-MCF) at different pH values were found to vary greatly (Fig. 5b). The reaction catalyzed with free enzyme attained maximum conversion at 120 min and later tended to be reversible at higher pH values of 8 and 8.5. Whereas, reaction with immobilized PGA reached maxima at 180 min and was irreversible at all pH range tested. Thus pH 7 was used for the further study.

3.11. Effect of temperature

The next intrinsic parameter tested was the reaction temperature. Immobilized PGA had higher activity than a free enzyme, but the trend remained the same for both. The conversion increased with temperature and reached maxima at 50 °C. Conversion dropped for immobilized PGA but remained stable for the free enzyme at 60 °C (Fig. 5c). Immobilized PGA from reaction carried out at 60 °C was recovered and reused at 40 °C, at which regain in activity was observed. Hence, loss of activity at higher temperature is attributed to irreversible PGA inactivation. The reaction temperature of 50 °C was chosen for further study. Overall higher conversion by the enzyme on immobilization could be attributed to either improvement in the activity or reduction in enzyme deactivation or reduction in negative feedback by the products. To decipher it more, we calculated the energy of activation from Arrhenius plots (Fig. 5d). The energy of activation for the free enzyme was 6.35 kcal mol^{-1} and for PVA/SA-Crs-Enz-NH_2-MCF was 8.42 kcal mol^{-1}. These values are reasonable for enzymatic reactions. The higher energy of activation for beads means there is more temperature dependence and the rate of reaction changes significantly for beads than that for the free enzyme with a change in temperature. It also reflects the diffusional limitation of the substrate in immobilized PGA.

3.12. Enzyme reusability and thermal stability

The aim of our study was to improve the reusability of the biocatalyst making the process economical. To prove the advantage of PGA immobilized beads over the previous step of immobilization (Crs-Enz-NH_2-MCF), catalyst reusability study was carried out for both (Fig. 6a). Reusability was determined for five cycles with similar reaction conditions. Crs-Enz-NH_2-MCF addition was done on activity equivalent basis. SA/PVA-Crs-Enz-NH_2-MCF had better reusability than Crs-Enz-NH_2-MCF (Fig. 6a). The formation of polymer matrix layer entrapping PGA immobilized foam particles prevented leaching of the enzyme. The protein estimation of reaction mixture filtrate was also done to verify leaching. PVA/SA-Crs-Enz-NH_2-MCF retained 94.3% activity retention even after fifth use (and 80% after 10th use) where Crs-Enz-NH_2-MCF lost half of its activity after fifth use.

To study the thermal stability (Fig. 6b) of biocatalysts, they were subjected to 50° C in phosphate buffer (10 mM, pH 7) under static conditions for a few days until the activity drop was significant. Free

Table 1
Surface area and pore characteristics of different stages of penicillin G acylase immobilization.

Steps →	1	2	3	4	5
Parameter	MCF	NH_2-MCF	Crs-Enz-NH_2-MCF	SA/PVA- Crs-Enz-NH_2-MCF	Permeabilized SA/PVA- Crs-Enz-NH_2-MCF
BET surface area ($m^2 g^{-1}$)	605.4	484.6	203.6	193.0	158.5
Pore volume (BJH adsorption) ($cm^3 g^{-1}$)	3.2	3.3	0.7	0.6	0.6
Pore size (BJH adsorption) (nm)	28.0	33.1	13.5	13.8	15.0

Table 2
Immobilization parameters for biocatalysts (refer section 3.1).

	Mode/s of immobilization	Immobilization yield (% w/w)	% Activity retained	% Enzyme deactivation
Enz-MCF	Adsorption	38.3	36.7	1.6
Crs-Enz-MCF	Adsorption followed by crosslinking	76.8	70.0	6.8
Enz-NH_2-MCF	Covalent attachment	66.1	63.3	2.8
Crs-Enz-NH_2-MCF	Covalent attachment followed by crosslinking	97.8	91.7	6.1
SA/PVA-Crs-Enz-NH_2-MCF	Covalent attachment followed by crosslinking followed by entrapment	97.8	94.8	3.0

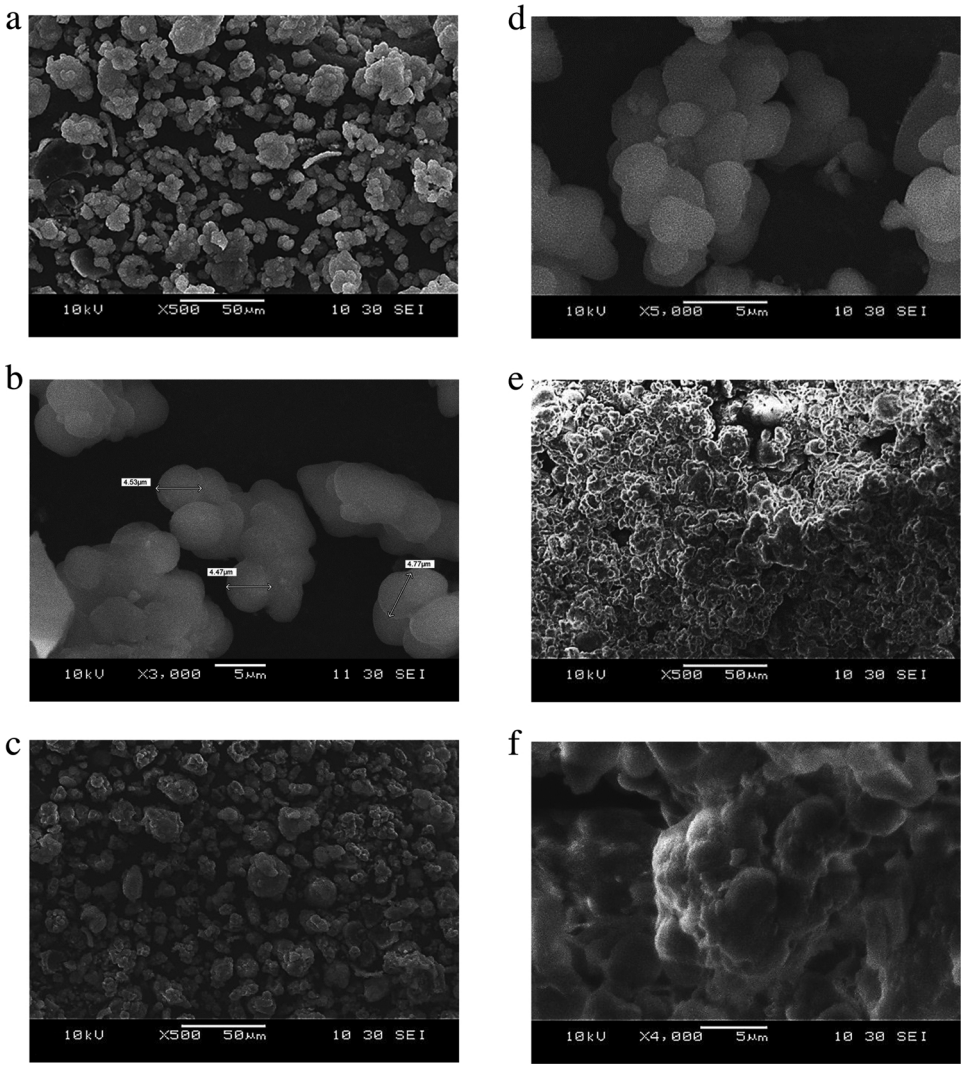

Fig. 3. SEM image (a) MCF. (b) MCF. (c) Crs-Enz-NH_2-MCF. (d) Crs-Enz-NH_2-MCF. (e) SA/PVA-Crs-Enz-NH_2-MCF. (f) SA/PVA-Crs-Enz-NH_2-MCF.

enzyme lost 90% activity in 24 h. SA/PVA-Crs-Enz-NH_2-MCF and Crs-Enz-NH_2-MCF retained 68% and 55% of their activity respectively until the 7th day suggesting improvement in the thermal stability due to immobilization.

3.13. Effect of substrate concentration

The enzymatic action of PGA involves two reactants- penicillin G salt and water. Water being solvent, is in excess and penicillin G salt is the limiting reactant. The conversion and reaction rate decreased with an increase in the concentration of penicillin G due to the inhibitory effect of substrate on biocatalyst [5] (Fig. 7a and 7b). This inhibitory effect is more dominant in the case of free enzyme than SA/PGA-Crs-Enz-NH_2-MCF. At low concentration (10 mM) of penicillin G, the free enzyme showed more activity and conversion. At higher penicillin G concentration (30 and 50 mM), the PGA/SA-Crs-Enz-NH_2-MCF had more conversion and activity. This suggests that the immobilized enzyme has increased resistance to the substrate inhibition even at higher substrate loading. The lower activity at a low concentration of substrate can be justified by diffusional limitations that were even evident from Arrhenius plot. The reaction of hydrolysis is highly selective, and no other side-products were seen. Conversion decreased with increasing substrate concentration in both cases (Table 3).

3.14. Reaction kinetics

Initial rates of reactions were determined for varying substrate concentration. PGA is non- competitively inhibited by the substrate-

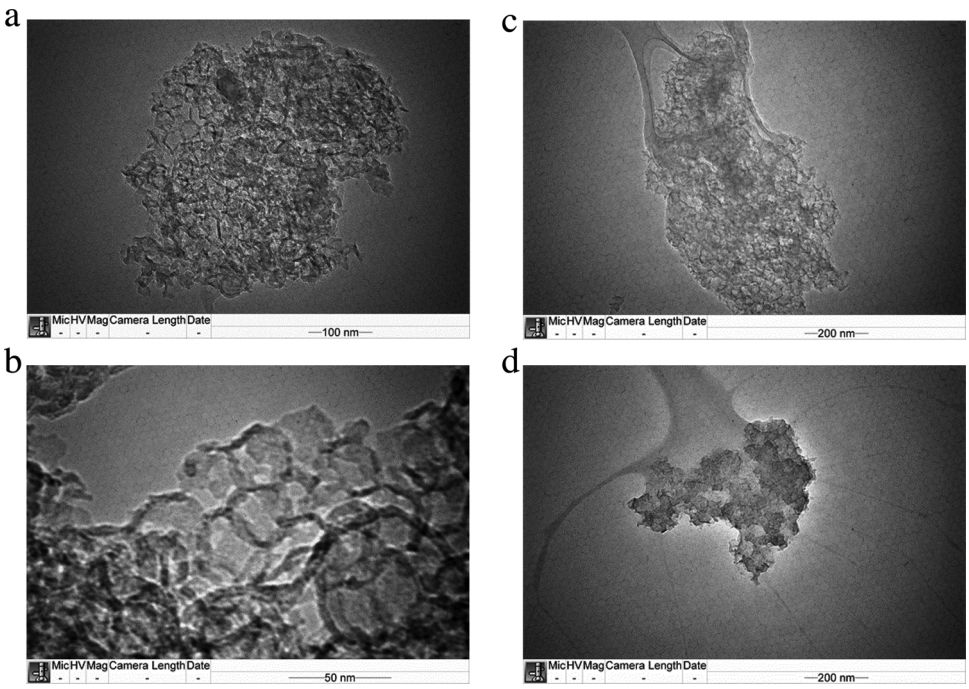

Fig. 4. TEM images (a) Crs-Enz-NH_2-MCF. (b) Crs-Enz-NH_2-MCF. (c) SA/PVA-Crs-Enz-NH_2-MCF. (d) SA/PVA-Crs-Enz-NH_2-MCF.

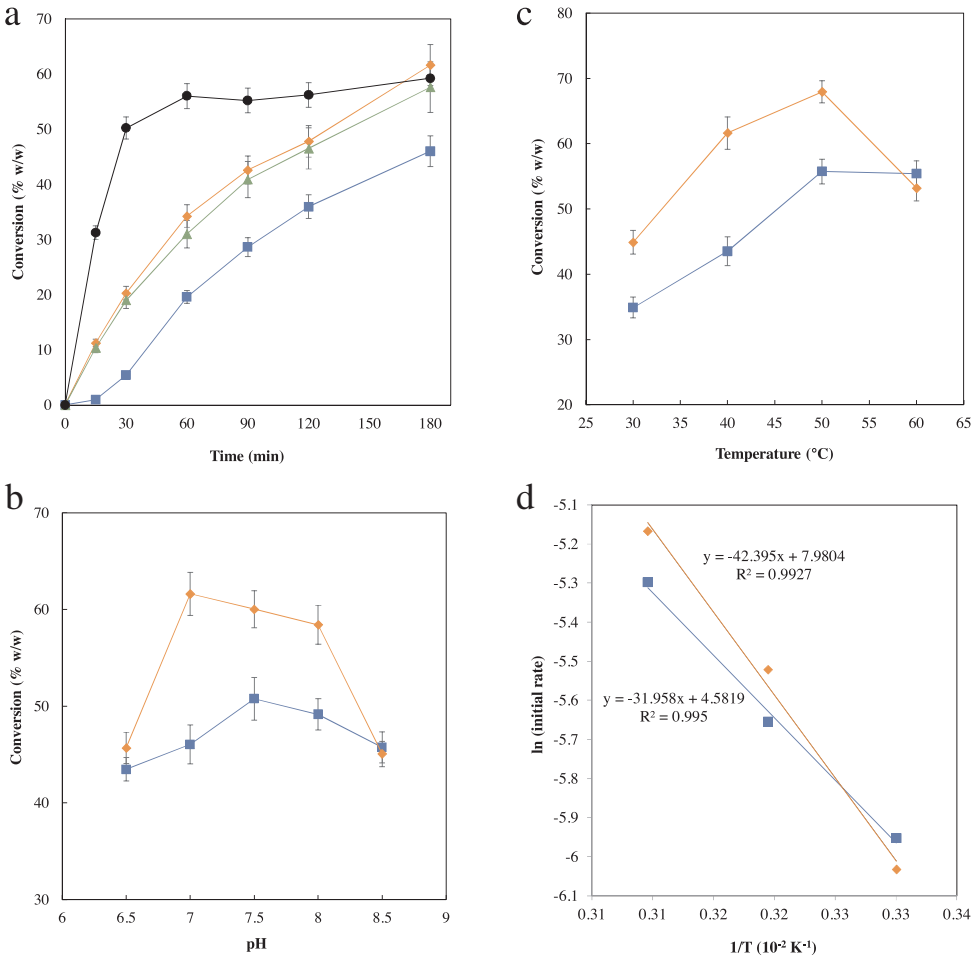

Fig. 5. (a) Effect of speed of agitation on SA/PVA-Crs-Enz-NH_2-MCF reaction progress. Speeds of agitation: ■ 150 rpm, ◆ 200 rpm, ▲ 250 rpm and ● 300 rpm. (b) Effect of pH of the reaction mixture on penicillin G hydrolysis progress catalyzed by ■ free enzyme and by ◆ SA/PVA-Crs-Enz-NH_2-MCF. (c) Effect of temperature on penicillin G hydrolysis reaction catalyzed by ■ free enzyme and by ◆ SA/PVA-Crs-Enz-NH_2-MCF. (d) Arrhenius plots. ■ Free enzyme and by ◆ SA/PVA-Crs-Enz-NH_2-MCF.

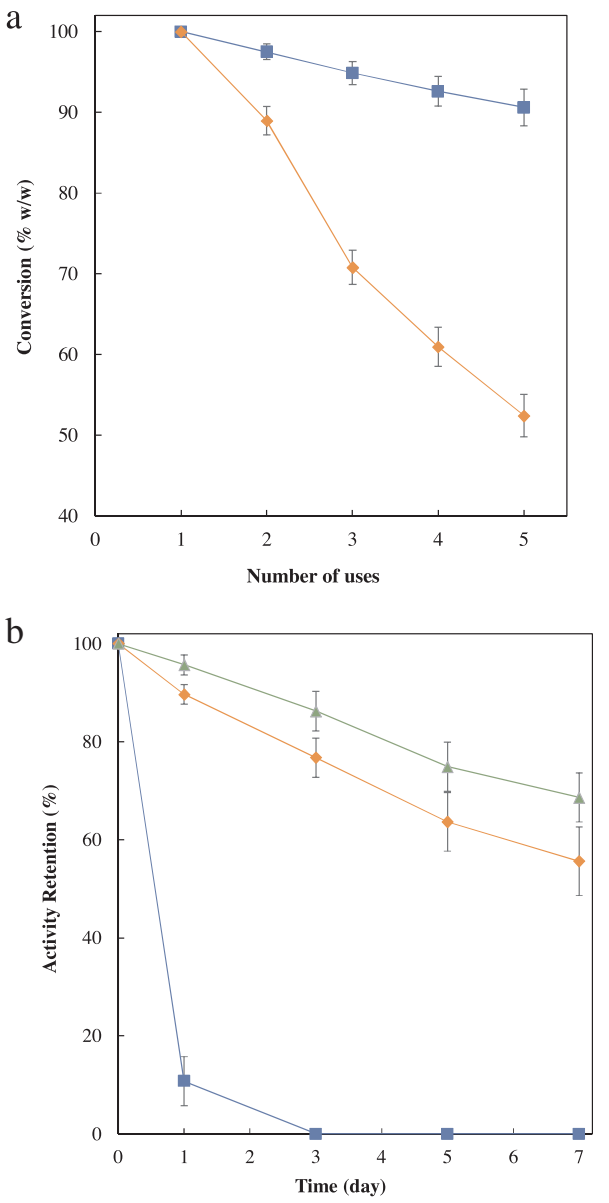

Fig. 6. (a) Reusability of biocatalyst. ■ SA/PVA-Crs-Enz-NH_2-MCF and by ◆ Crs-Enz-NH2-MCF. (b) Thermal stability of biocatalysts. ■ Free enzyme, ◆ Crs-Enz-NH_2-MCF and ▲ SA/PVA-Crs-Enz-NH_2-MCF.

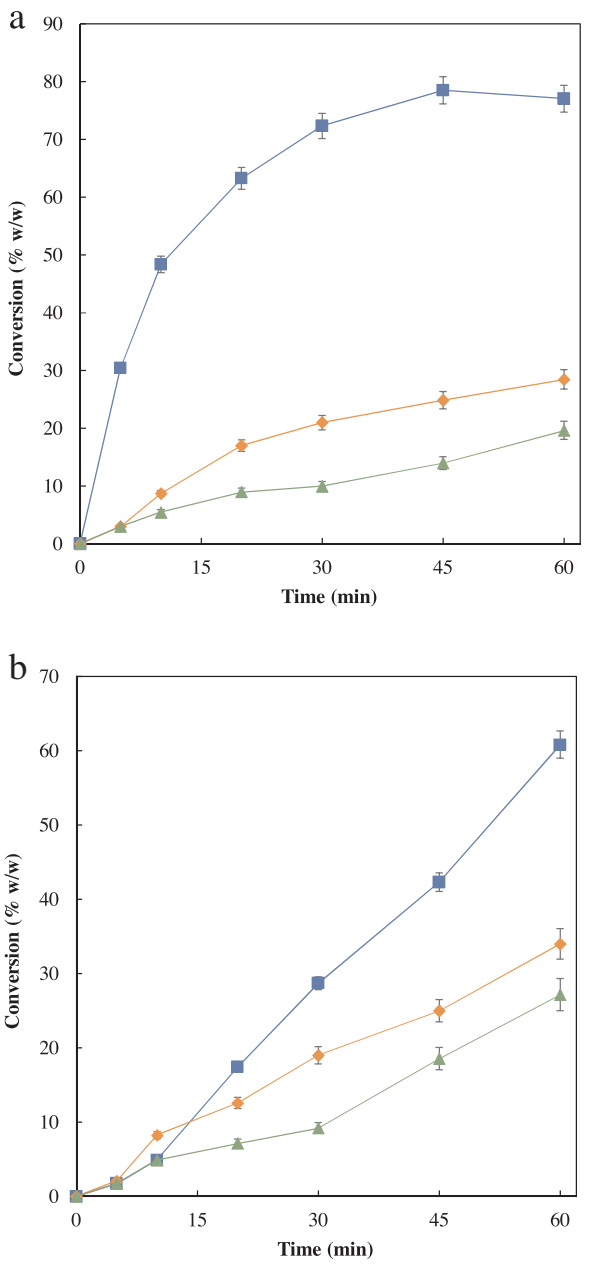

Fig. 7. (a) Initial rates of penicillin G hydrolysis reactions catalyzed by free enzyme at penicillin G concentrations: ■ 10 mM, ◆ 20 mM and ▲ 30 mM. (b) Initial rates of penicillin G hydrolysis reactions catalyzed by SA/PVA-Crs-Enz-NH_2-MCF at penicillin G concentrations: ■ 10 mM, ◆ 20 mM and ▲ 30 mM.

penicillin G [5] and Lineweaver Burk (Fig. 8a) plots for free and immobilized PGA did not cross at the same point. Michaelis Menten constants (K_m) for free and immobilized enzyme were 20.71 mM^{-3} and 19.31 mM, respectively. The low value of Km suggests that immobilized enzyme has more affinity than that of free enzyme towards the substrate. Maximum velocity of reaction (V_{max}) is 0.38 mM min^{-1} and 0.29 mM min^{-1}. For all these experiments the enzyme concentration was 0.2 IU. cm^{-3} of the reaction mixture.

Usually hydrolysis reactions are treated as uni-bi reactions [42] indicating that one reactant gives rise to two products, when carried out in aqueous solutions. The proposed reaction rate equation is as follows:

$$A + B \xrightarrow{E} P + Q \quad (1)$$

For the above reaction,

$$A + E \overset{K_A}{\longleftrightarrow} A.E \quad (2)$$

$$B + E \overset{K_B}{\longleftrightarrow} B.E \quad (3)$$

Table 3
Yield of 6-amino penicillanic acid.

Penicillin G concentration		Yield (mg of 6-APA per 30 mL of the reaction mixture)	
mM	mg of Penicillin G per 30 cm^3 of the reaction mixture	Free Enzyme	SA/PGA-Crs-Enz-NH_2-MCF
10	112.0	86.2	68.1
30	335.0	95.5	113.9
50	559.0	109.6	152.0

$$A.E + B.E \overset{K_1}{\leftrightarrow} P.E + Q.E \quad (4)$$

$$P.E \underset{K_P}{\leftrightarrow} P + E \quad (5)$$

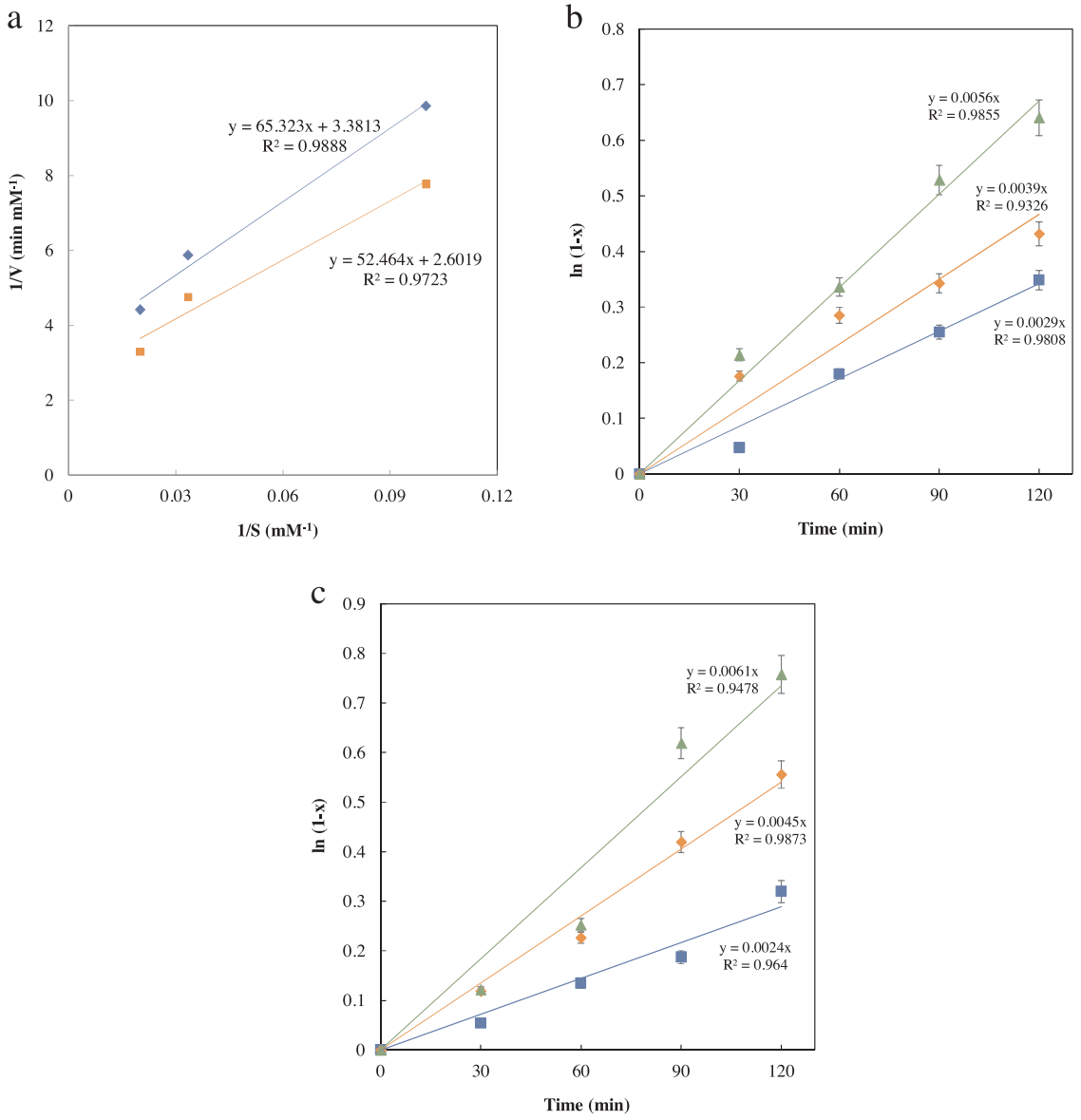

Fig. 8. (a) Lineweaver Burk plot for ◆ free enzyme and ■ SA/PVA-Crs-Enz-NH_2-MCF. V: initial rate or velocity of the reaction, S: substrate-penicillin G acylase concentration. (b) Reaction rate plot for free enzyme at temperatures: ■ 30 °C, ◆ 40 °C and ▲ 50 °C. x is fractional conversion of penicillin G. (c) Reaction rate plot for SA/PVA-Crs-Enz-NH_2-MCF at temperatures: : ■ 30 °C, ◆ 40 °C and ▲ 50 °C. x is fractional conversion of penicillin G.

$$Q.\,E \underset{K_Q}{\longleftrightarrow} Q + E \tag{6}$$

Rate expression for the overall reaction can be written as,

$$-r_A = k^{'} C_{A.E}\, C_{B.E} - k_1^{'} C_{P.E}\, C_{Q.E} \tag{7}$$

Also, the total catalytic sites,

$$C_t = C_{A.E} + C_{B.E} + C_{P.E} + C_{Q.E} + C_E \tag{8}$$

Substituting this in the rate expression (8) we get,

$$-r_A = \frac{C_t^2 (k_1 K_A K_B C_A C_B - k_1' K_P K_Q C_P C_Q)}{(1 + K_A C_A + K_B C_B + K_P C_P + K_Q C_Q)} \tag{9}$$

Only initial rate is considered when adsorption is weak, the concentration of reactants is very large than that of products and therefore, substrate inhibition can also be ignored.

$$-r_{initial} = k\, C_A\, C_B \tag{10}$$

Where,

$$k = k"e;\, w \tag{11}$$

Expression 9 becomes,

$$-r_{initial} = \frac{C_t^2\, k_I K_A K_B\, C_A\, C_B}{(1 + K_A\, C_A + K_B\, C_B)^2} \tag{12}$$

Since, K_A and $K_B < < < 1$, hence $(1 + K_A\, C_A + K_B\, C_B)$ is almost equal to 1

Also, B is in excess, hence,

$$-r_{initial} = k\, C_A \tag{13}$$

Here, $k = C_t^2\, k_1\, k_A\, k_B$

Hence, for the initial kinetically controlled reaction of penicillin G hydrolysis using PGA can be deduced to first (pseudo-first) order reaction mechanism. Initial reaction rate plots (Fig. 8b and 8c) verified that both free and immobilized PGA (SA/PGA-Crs-Enz-NH_2-MCF) exhibited first order rate kinetics. The apparent rate constants were calculated and reported in Table 4. A higher value of the apparent rate constant for SA/PGA-Crs-Enz-NH_2-MCF indicated a faster reaction.

Table 4
Kinetic constants for penicillin G hydrolysis reaction.

Temperature (°C)	Free Enzyme		SA/PGA-Crs-Enz-NH_2-MCF	
	k (min^{-1})	k" ($cm^3\,g^{-1}\,min^{-1}$)	k (min^{-1})	k" ($cm^3\,g^{-1}\,min^{-1}$)
30	0.0029	126.08	0.0024	0.24
40	0.0039	169.56	0.0045	0.45
50	0.0056	243.47	0.0061	0.61

4. Conclusions

Support of siliceous foam entrapped in the polymer matrix was developed. A systematic study was undertaken to understand the role of each component. Penicillin acylase was covalently immobilized on aminopropyl functionalized mesocellular foam and was further cross-linked using glutaraldehyde, which was highly stable and active, with only 3% deactivation and 94.8% efficiency. At this step, 140.8 g of protein loading and 1185 IU of penicillin acylase activity was obtained per gram of foam. Mesocellular foam silica (MCF) has high porosity and wide interconnected pore structures, and hence has a disadvantage of enzyme leaching. Hence it was then entrapped into polyvinyl alcohol (5%) – alginate (2%) bead with a polymer to enzyme immobilized foam ratio of 2:1 volumetrically. The enzymatic activity was 20 IU/g- beads. Enzyme immobilization increased penicillin G conversion from 56% to 68%. The immobilized enzyme also showed improved resistance to substrate inhibition and exhibited an absence of reversible reaction at high pH (above 8) unlike free enzyme. All these improvements in intrinsic parameters were the result of favorable conformational changes induced and resistance to deactivation mechanisms due to immobilization. The immobilized enzyme in bead showed improved pH stability and highest thermal activity at 50 °C. Both enzyme immobilized foam and the foam entrapped bead showed the same conversion on first use without much difference in rate indicating the absence of diffusional limitations. But, the activity of foam decreased to 52.4% due to enzyme leaching whereas, 90.6% enzyme activity was retained for beads. Beads had improved thermal stability and could be stored with 70% retention of activity for a week at elevated temperature. The novel supported biocatalyst was characterized at each step. Finally, a rate expression was also deduced for penicillin G hydrolysis to 6-APA and kinetic parameters were calculated. This is an example of biocatalysis where smart construction of the immobilized enzyme not only yielded improved physical parameters but also reduced mechanisms of enzyme deactivation of catalytic promiscuity.

Declaration of Competing Interest

The authors declare no conflict of interest.

Acknowledgements

S.R.A. acknowledges junior research fellowship (DBT, GoI). G.D.Y. gratefully acknowledges support as R.T. Mody Distinguished Professor Tata Chemicals Darbari Seth Distinguished Professor of Leadership and Innovation and J.C. Bose National Fellow (DST, GoI).

References

[1] Z. Ashraf, A. Bais, M.M. Manir, U. Niazi, Novel penicillin analogues as potential antimicrobial agents; design, synthesis and docking studies, PLoS One 10 (2015) e0135293, , https://doi.org/10.1371/journal.pone.0135293.
[2] M. Grulich, V. Štěpánek, P. Kyslík, Perspectives and industrial potential of PGA selectivity and promiscuity, Biotechnol. Adv. 31 (2013) 1458–1472, https://doi.org/10.1016/j.biotechadv.2013.07.005.
[3] H.W.O. Weissenburger, M.G. van der Hoeven, An efficient nonenzymatic conversion of benzylpenicillin to 6-aminopenicillanic acid, Recl. Des Trav. Chim. Des Pays-Bas. 89 (1970) 1081–1084, https://doi.org/10.1002/recl.19700891011.
[4] A.P. Dicks, A. Hent, Atom economy and reaction mass efficiency, Green Chemistry Metrics: A Guide to Determining and Evaluating Process Greenness, Springer, 2015, https://link.springer.com/book/10.1007%2F978-3-319-10500-0.
[5] J. Rajendhran, P. Gunasekaran, Recent biotechnological interventions for developing improved penicillin G acylases, J. Biosci. Bioeng. 97 (2004) 1–13, https://doi.org/10.1016/S1389-1723(04)70157-7.
[6] S. Deng, X. Ma, E. Su, D. Wei, Efficient cascade synthesis of ampicillin from penicillin G potassium salt using wild and mutant penicillin G acylase from *Alcaligenes faecalis*, J. Biotechnol. 219 (2016) 142–148, https://doi.org/10.1016/j.jbiotec.2015.12.034.
[7] R. Virden, Structure, Processing and catalytic action of penicillin acylase, Biotechnol. Genet. Eng. Rev. 8 (1990) 189–218, https://doi.org/10.1080/02648725.1990.10647869.
[8] R. Liu, D. Chen, H. Fu, P. Lv, D. Zhang, Y. He, A facile preparation process of magnetic aldehyde-functionalized $Ni_{0.5}$ $Zn_{0.5}$ Fe_2O_4 @SiO_2 nanocomposites for immobilization of penicillin g acylase (PGA), J. Nanosci. Nanotechnol. 17 (2017) 893–899, https://doi.org/10.1166/jnn.2017.12694.
[9] B. Zhang, J. Wang, J. Chen, H. Zhang, D. Yin, Q. Zhang, Magnetic mesoporous microspheres modified with hyperbranched amine for the immobilization of penicillin G acylase, Biochem. Eng. J. 127 (2017) 43–52, https://doi.org/10.1016/j.bej.2017.07.011.
[10] V.S. Avinash, P.D. Chauhan, S. Gaikwad, A. Pundle, Biotransformation of penicillin V to 6-aminopenicillanic acid using immobilized whole cells of *E. coli* expressing a highly active penicillin V acylase, Prep. Biochem. Biotechnol. 47 (2017) 52–57, https://doi.org/10.1080/10826068.2016.1163580.
[11] X. Li, L. Tian, Z. Ali, W. Wang, Q. Zhang, Design of flexible dendrimer-grafted flower-like magnetic microcarriers for penicillin G acylase immobilization, J. Mater. Sci. 53 (2018) 937–947, https://doi.org/10.1007/s10853-017-1581-9.
[12] D. Liu, Z. Chen, J. Long, Y. Zhao, X. Du, Immobilization of penicillin acylase on macroporous adsorption resin CLX1180 carrier, Adv. Polym. Technol. 37 (2018) 753–760, https://doi.org/10.1002/adv.21717.
[13] K. Li, X.T. Liu, Y.F. Zhang, D. Liu, X.Y. Zhang, S.M. Ma, J.M. Ruso, Z. Tang, Z. Bin Chen, Z. Liu, The engineering and immobilization of penicillin G acylase onto thermo-sensitive tri-block copolymer system, Polym. Adv. Technol. 30 (2019) 86–93, https://doi.org/10.1002/pat.4446.
[14] Y.D. Ahn, J.H. Lee, Development of a polyaniline-coated monolith reactor for the synthesis of cephalexin using penicillin g acylase aggregates, Biotechnol. Bioprocess Eng. 23 (2018) 349–354, https://doi.org/10.1007/s12257-018-0124-9.
[15] H. Shi, Y. Wang, G. Luo, Preparation and enzymatic activity of penicillin G acylase immobilized on core-shell porous glass beads, J. Mol. Catal. B Enzym. 106 (2014) 40–45, https://doi.org/10.1016/j.molcatb.2014.04.013.
[16] K. Li, Z. Bin Chen, D.L. Liu, L. Zhang, Z. Tang, Z. Wang, Y. Zhao, Z. Liu, Design and synthesis study of the thermo-sensitive copolymer carrier of penicillin G acylase, Polym. Adv. Technol. 29 (2018) 1902–1912, https://doi.org/10.1002/pat.4299.
[17] X. Li, L. Tian, Z. Ali, W. Wang, Q. Zhang, Design of flexible dendrimer-grafted flower-like magnetic microcarriers for penicillin G acylase immobilization, J. Mater. Sci. 53 (2018) 937–947, https://doi.org/10.1007/s10853-017-1581-9.
[18] Q. Yu, Z. Wang, Y. Zhang, R. Liu, Covalent immobilization and characterization of penicillin G acylase on amino and GO functionalized magnetic $Ni_{0.5}Zn_{0.5}Fe_2O_4$@SiO_2 nanocomposite prepared via a novel rapid-combustion process, Int. J. Biol. Macromol. 134 (2019) 507–515, https://doi.org/10.1016/j.ijbiomac.2019.05.066.
[19] B. Zhang, J. Wang, J. Chen, H. Zhang, D. Yin, Q. Zhang, Magnetic mesoporous microspheres modified with hyperbranched amine for the immobilization of penicillin G acylase, Biochem. Eng. J. 127 (2017) 43–52, https://doi.org/10.1016/J.BEJ.2017.07.011.
[20] Z.X. Huang, S.L. Cao, P. Xu, H. Wu, M.H. Zong, W.Y. Lou, Preparation of a novel nanobiocatalyst by immobilizing penicillin acylase onto magnetic nanocrystalline cellulose and its use for efficient synthesis of cefaclor, Chem. Eng. J. 346 (2018) 361–368, https://doi.org/10.1016/j.cej.2018.04.026.
[21] X. Chen, L. Yang, W. Zhan, L. Wang, Y. Guo, Y. Wang, G. Lu, Y. Guo, Immobilization of penicillin G acylase on paramagnetic polymer microspheres with epoxy groups, Cuihua Xuebao/Chinese J. Catal. 39 (2018) 47–53, https://doi.org/10.1016/S1872-2067(17)62934-6.
[22] A. Arsalan, H. Younus, Enzymes and nanoparticles: modulation of enzymatic activity via nanoparticles, Int. J. Biol. Macromol. 118 (2018) 1833–1847, https://doi.org/10.1016/j.ijbiomac.2018.07.030.
[23] A. Kołodziejczak-Radzimska, J. Zdarta, T. Jesionowski, Physicochemical and catalytic properties of acylase I from *Aspergillus melleus* immobilized on amino- and carbonyl-grafted stöber silica, Biotechnol. Prog. 34 (2018) 767–777, https://doi.org/10.1002/btpr.2610.
[24] B. Chayasombat, S. Fearn, C. Thanachayanont, S. Prichanont, A. Phongphut, N. Thananukul, A comparative study on mesocellular foam silica with different template removal methods and their effects on enzyme immobilization, J. Porous Mater. (2018) 1–10, https://doi.org/10.1007/s10934-018-0705-1.
[25] J. Zhao, Y. Wang, G. Luo, S. Zhu, Covalent immobilization of penicillin G acylase on aminopropyl-functionalized mesostructured cellular foams, Bioresour. Technol. 101 (2010) 7211–7217, https://doi.org/10.1016/j.biortech.2010.04.067.
[26] Z. Gao, W. Zhan, Y. Wang, Y. Guo, L. Wang, Y. Guo, G. Lu, Aldehyde-functionalized mesostructured cellular foams prepared by copolymerization method for immobilization of penicillin G acylase, Microporous Mesoporous Mater. 202 (2015) 90–96, https://doi.org/10.1016/j.micromeso.2014.09.053.
[27] C.E. McVey, M.A. Walsh, G.G. Dodson, K.S. Wilson, J.A. Brannigan, Crystal structures of penicillin acylase enzyme-substrate complexes: structural insights into the catalytic mechanism, J. Mol. Biol. 313 (2001) 139–150, https://doi.org/10.1006/jmbi.2001.5043.
[28] Y. Lü, Y. Guo, Y. Wang, X. Liu, Y. Wang, Y. Guo, Z. Zhang, G. Lu, Immobilized

penicillin G acylase on mesoporous silica: the influence of pore size, pore volume and mesophases, Microporous Mesoporous Mater. 114 (2008) 507–510, https://doi.org/10.1016/J.MICROMESO.2007.12.027.
[29] P.A. Russo, M.M.L. Ribeiro Carrott, P.A.M. Mourão, P.J.M. Carrott, Tailoring the surface chemistry of mesocellular foams for protein adsorption, Colloids Surf. A Physicochem. Eng. Asp. 386 (2011) 25–35, https://doi.org/10.1016/j.colsurfa.2011.06.022.
[30] P. Schmidt-Winkel, W.W. Lukens, P. Yang, D.I. Margolese, J.S. Lettow, J.Y. Ying, G.D. Stucky, Microemulsion templating of siliceous mesostructured cellular foams with well-defined ultralarge mesopores, Chem. Mater. 12 (2000) 686–696, https://doi.org/10.1021/cm991097v.
[31] N. Balistreri, D. Gaboriau, C. Jolivalt, F. Launay, Covalent immobilization of glucose oxidase on mesocellular silica foams: characterization and stability towards temperature and organic solvents, J. Mol. Catal., B Enzym. 127 (2016) 26–33, https://doi.org/10.1016/j.molcatb.2016.02.003.
[32] P. Schmidt-Winkel, W.W. Lukens, D. Zhao, P. Yang, B.F. Chmelka, G.D. Stucky, Mesocellular siliceous foams with uniformly sized cells and windows, J. Am. Chem. Soc. 121 (1999) 254–255, https://doi.org/10.1021/ja983218i.
[33] H. Sun, X.Y. Bao, X.S. Zhao, Immobilization of penicillin G acylase on oxirane-modified mesoporous silicas, Langmuir 25 (2009) 1807–1812, https://doi.org/10.1021/la803480c.
[34] F. López-Gallego, J.M. Guisán, L. Betancor, Glutaraldehyde-mediated protein immobilization, Methods Mol. Biol. 1051 (2013) 33–41, https://doi.org/10.1007/978-1-62703-550-7_3.
[35] L. Zhou, X. Luo, J. Li, L. Ma, Y. He, Y. Jiang, L. Yin, L. Gao, Meso-molding three-dimensionally ordered macroporous alumina: a new platform to immobilize enzymes with high performance, Biochem. Eng. J. 146 (2019) 60–68, https://doi.org/10.1016/j.bej.2019.03.002.
[36] S.D. Gür, N. İdil, N. Aksöz, Optimization of enzyme Co-immobilization with sodium alginate and glutaraldehyde-activated chitosan beads, Appl. Biochem. Biotechnol. 184 (2017) 1–15, https://doi.org/10.1007/s12010-017-2566-5.
[37] A. Sassolas, A. Hayat, J.L. Marty, Enzyme immobilization by entrapment within a gel network, Methods Mol. Biol. 1051 (2013) 229–239, https://doi.org/10.1007/978-1-62703-550-7_15.
[38] B. Bhushan, A. Pal, V. Jain, Improved enzyme catalytic characteristics upon glutaraldehyde cross-linking of alginate entrapped xylanase isolated from *Aspergillus flavus MTCC 9390*, Enzyme Res. 2015 (2015) 210784, , https://doi.org/10.1155/2015/210784.
[39] V.V. Vinogradov, D. Avnir, Exceptional thermal stability of therapeutical enzymes entrapped in alumina sol–gel matrices, J. Mater. Chem. B Mater. Biol. Med. 2 (2014) 2868, https://doi.org/10.1039/c3tb21643h.
[40] M.P. Kamble, S.D. Shinde, G.D. Yadav, Kinetic resolution of (R,S)-α-tetralol catalyzed by crosslinked Candida antarctica lipase B enzyme supported on mesocellular foam: a nanoscale enzyme reactor approach, J. Mol. Catal., B Enzym. 132 (2016) 61–66, https://doi.org/10.1016/j.molcatb.2016.06.013.
[41] Z.D. Knežević-Jugovic, M.G. Žuža, S.M. Jakovetić, A.B. Stefanović, E.S. Džunuzović, K.B. Jeremić, S.M. Jovanović, An approach for the improved immobilization of penicillin G acylase onto macroporous poly(glycidyl methacrylate-co-ethylene glycol dimethacrylate) as a potential industrial biocatalyst, Biotechnol. Prog. 32 (2016) 43–53, https://doi.org/10.1002/btpr.2181.
[42] W.W. Cleland, The kinetics of enzyme-catalyzed reactions with two or more substrates or products. III. Prediction of initial velocity and inhibition patterns by inspection, Biochim. Biophys. Acta 67 (1963) 188–196 http://www.ncbi.nlm.nih.gov/pubmed/14021669.